Angewandte Chemie
Eine Zeitschrift der Gesellschaft Deutscher Chemiker

Supporting Information

Chemoselective Alteration of Fluorophore Scaffolds as a Strategy for the Development of Ratiometric Chemodosimeters

*Xinqi Zhou, Lauren Lesiak, Rui Lai, Jon R. Beck, Jia Zhao, Christian G. Elowsky, Hui Li, and Cliff I. Stains**

anie_201612628_sm_miscellaneous_information.pdf

Table of Contents

General Experimental Details

Reagents and Instrumentation

All reactions were performed in oven-dried glassware charged with nitrogen unless otherwise noted. All the reagents and solvents were directly used as commercially supplied without further purification. Anhydrous THF was prepared using 3 Å molecular sieves.[1] Reaction progress was monitored by either thin layer chromatography (TLC) or high performance liquid chromatography (HPLC). Products were purified by flash chromatography using Merck silica gel 60 (230-400 mesh). Prep HPLC purification was done with a semi-prep column (YMC-Pack ODS-A，5 μm, 250×20 mm). Mass spectra were recorded by electrospray ionization mass spectrometry (ESI, Thermo Finnigan LCQ Advantage). High-resolution mass spectrometry (HRMS) was performed by the Nebraska Center for Mass Spectrometry. Mass data are reported in units of m/z for $[M+H]^+$ or $[M+Na]^+$. ^{1}H NMR and ^{13}C NMR were performed in $CDCl_3$ at room temperature and the spectra were recorded using Bruker-DRX-Avance 300 or 400 MHz instruments. Chemical shifts are reported relative to $CDCl_3$ (7.26 ppm for ^{1}H NMR and 77.0 ppm for ^{13}C NMR). For ^{11}B NMR, boron trifluoride diethyl etherate in $CDCl_3$ was used as an external standard (0.00 ppm). Fluorescence spectra were recorded using a FluoroMax-4 spectrofluorometer (Horiba Scientific) in either a 100 μL or 3 mL quartz cuvette. UV-Vis spectra were recorded using a BioMate 3S UV-Visible spectrophotometer (Thermo Scientific) in a 100 μL quartz cuvette. Near Infrared (NIR) fluorescence pictures were taken by a home-made full-spectrum digital single-lens reflex (DSLR) camera (Canon Rebel XSi) and a 720 nm NIR filter (Hoya 67 mm RM72 Infrared Filter) with an exposure time of 30 s. Confocal microscopy was performed with a Nikon A1 confocal system on a Nikon 90i upright fluorescence microscope. Laser lines included blue (excitation: 405 nm, emission filter: 425 nm — 475 nm), green (excitation: 490 nm, emission filter: 500 nm — 530 nm), red (excitation: 560 nm, emission filter: 560 nm — 617 nm) and deep red (excitation: 640 nm, emission filter: 663 nm — 738 nm). Images for quantification were obtained using identical instrument parameters for each sample. ImageJ software was used for data analysis.

Computational Methods

Density functional theory (DFT) and time-dependent DFT (TDDFT)[2] calculations were performed using the Quantum chemistry Polarizable force field program (QuanPol)[3] integrated in the General Atomic and Molecular Electronic Structure System (GAMESS)[4] package. The B3LYP[5] functional and 6-31++G(d,p)[6] basis set was used for both DFT and TDDFT calculations. The water solvent was described by using the FixSol[7] solvation model with a

dielectric constant of 78.39. We optimized the S_0 ground state geometries of TMR, **RF_{620}**, SiR, and **SiOH2R** using B3LYP, and performed single point energy calculations using TD-B3LYP to obtain the HOMO and LUMO energies as well as the vertical excitation energies (S_0->S_n). S_1 excited state geometries were then optimized using TD-B3LYP, and the S_1->S_0 de-excitation energies were calculated.

Molar Extinction Coefficient Measurement

Stock solutions were made by dissolving a solid sample in DMSO. Increasing concentrations of the sample were prepared (1, 2, 3, 4, and 5 μM) as well as a blank. Sample absorbance was measured and the molar extinction coefficient was determined by a linear fit of the absorbance versus sample concentration.

Quantum Yield Measurement

Fluorescence quantum yield was determined by the following equation:

$$\Phi_x = (\Phi_{ST} * A_{ST} * F_X * \eta_X^2) / (A_X * F_{ST} * \eta_{ST}^2)$$

Φ is the quantum yield; A is the absorbance at the excitation wavelength (A was kept at ≤0.05 during fluorescence measurements to avoid self-quenching), F is the fluorescence intensity at the excitation wavelength; η is the refractive index of the solvent. The subscripts $_{ST}$ and $_X$ refer to the standard and unknown respectively. Sulforhodamine 101 (Sigma S7635) was used as the fluorescence reference standard (ex: 576 nm, em: 591 nm, Φ: 0.95 in ethanol)[8] for TMR. Oxazine 170 perchlorate (Sigma, 372056) was used as the fluorescence reference standard (ex: 627 nm, em: 645 nm, Φ: 0.579 in ethanol)[9] for **RF_{620}**. Alexa Fluor® 660 NHS Ester (Molecular Probes, A20007) was used as the fluorescence reference standard (ex: 668 nm, em: 698 nm, Φ: 0.37 in PBS) for **SiOH2R**.

Kinetic Measurement

Sample (5 μM) in PBS (10 mM, pH = 7.4 with 0.05% DMSO) was spiked with different concentrations of H_2O_2 and the cuvette was sealed with parafilm and placed in a fluorometer. Samples was continuously exposed to the excitation light during the experiment with an excitation slit width of 1 nm.

Selectivity Assay

All ROS solutions were prepared according to the previous literature.[10] **RF_{620}** and **SiOH2R** were kept at 10 μM in PBS (10 mM, pH = 7.4 with 0.1% DMSO). The concentration of HOCl and superoxide was kept at 20 μM and all the other ROS concentrations were kept at 200 μM.

Superoxide dismutase (SOD) and catalase were used to verify off-target signal generated by superoxide decomposition. Assays were performed in a 96-well plate with each ROS sample prepared and measured in triplicate. A PBS solution (200 µL) containing the sensors and ROS with a 70 µL mineral oil overlay to prevent evaporation, was placed in each well. The value of TMR/**RF_{620}** or TMR/**SiOH2R** was determined by dividing the fluorescence of TMR by the fluorescence of the indicated CAFS probe. Ratios determined at 5 minutes in the absence of H_2O_2 were set to 1.

Cell Imaging

HeLa cells (ATCC, CCL-2) were grown to 80% confluency in DMEM (Life Tech, 11965092) with 10% FBS (Life Tech, 16000036), 1x Pen/Strep (Life Tech, 15140122), and 1x Anti-Anti (Life Tech, 15240062). Media was then removed and replaced with pre-warmed (37 ºC) DMEM with HEPES and no phenol red (Life Tech, 2106245) with 10% FBS, 1x Pen/Strep, and 1x Anti-Anti for transportation. Media was subsequently removed and the cells were rinsed 3 times with prewarmed DPBS (Life Tech, 14040216). The cells were then incubated with DPBS containing reagents as indicated. All cells were washed three times before imaging.

Serum starved HeLa cells were prepared by changing the culture media to DMEM with 2 mM L-glutamine, 1x Pen/Strep (Life Tech, 15140122), and 1x Anti-Anti (Life Tech, 15240062) 12 h before imaging experiments.

Cell Toxicity Assay

HeLa cells (2×10^4) were incubated with the indicated concentration of **RF_{620}** and **SiOH2R** (containing 0.5% DMSO) for 6 h. Cells were then washed once with cell culture media (DMEM with 10% FBS, 1x Pen/Strep, and 1x Anti-Anti) and further incubated for 30 min. After washing, cell viability was assessed using the CellTiter-Glo 2.0 Assay (Promega).

Synthesis and Characterization of RF_{620} and SiOH2R

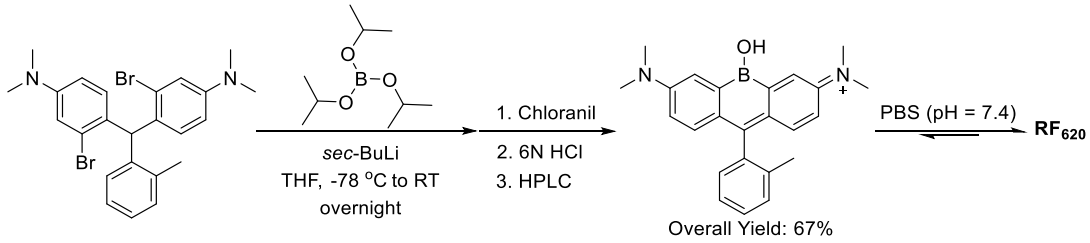

In a 50 mL flame dried round bottom flask, 4,4'-(o-tolylmethylene)bis(3-bromo-*N*,*N*-dimethylaniline)[11] (200 mg, 0.4 mmol, 1 eq) was dissolved in anhydrous THF (10 mL) and the flask was immersed in an acetone/dry ice bath to lower the temperature to -78 °C. After stirring at this temperature for 5 min, *sec*-Butyllithium (1.4 M in cyclohexane, 626 µL, 2.2 eq) was added dropwise through a 1 mL syringe and the reaction was further stirred for 1h. Triisopropyl borate (101 µL, 0.44 mmol, 1.1 eq) was then added dropwise and the reaction was stirred for another 3h at the same temperature. The acetone/dry ice bath was then replaced with an ice bath and the reaction was left overnight to allow the temperature to slowly reach room temperature. The next morning, the reaction was quenched by 2N HCl (10 mL) and the pH was adjusted to between 2 and 3 by adding saturated $NaHCO_3$ solution. The reaction was then extracted with dichloromethane (DCM) (3×100 mL) and the organic solution was combined and dried over sodium sulfate. After filtering and evaporating the solvent, the crude was dissolved in DCM (10 mL) and p-chloranil (294 mg, 1.2 mmol, 3 eq) was added. After stirring at room temperature for 30 min, the reaction temperature was lowered to 0 °C. The solution was filtered, washed with cold DCM, and the solvent was removed. The resulting dark blue solid was dissolved in 6N HCl (10 mL) and the orange solution was stirred at room temperature for 45 min. After filtering, the solvent was removed and the crude was dissolved in 8 mL HPLC buffer solution (50% acetonitrile / water with 0.1 % trifluoroacetic acid) and purified by HPLC. After lyophilization, 128 mg of a dark blue solid (yield: 67 %) was obtained. The borinic acid form of **RF_{620}** was directly used for structural characterization.

^{1}H NMR (300 MHz, $CDCl_3$) δ 7.43 – 7.26 (m, 3H), 7.22 (d, *J* = 7.5 Hz, 1H), 7.08 (d, *J* = 2.8 Hz, 2H), 7.02 (s, 1H), 6.99 (s, 1H), 6.42 (d, *J* = 2.8 Hz, 1H), 6.39 (d, *J* = 2.8 Hz, 1H), 3.20 (s, 12H), 2.15 (s, 3H).

^{13}C NMR (75 MHz, $CDCl_3$) δ 171.39, 155.52, 139.21, 138.35, 136.62, 129.70, 129.08, 128.69, 128.11, 124.90, 115.20, 111.74, 40.39, 19.44.

^{11}B NMR (96 MHz, $CDCl_3$) δ 1.74.

HRMS (EI) m/z calculated for $C_{24}H_{26}BN_2O^+$ $[M]^+$ 369.2133, found 369.2137.

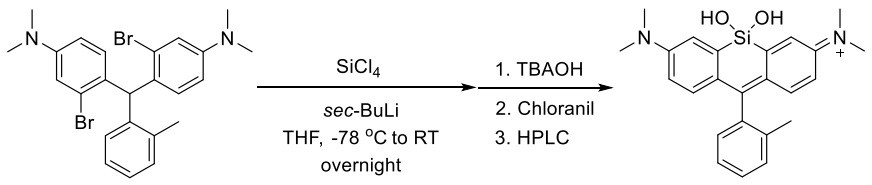

SiOH2R

Overall Yield: 20.3%

Similar to the synthesis of **RF_{620}**, 4,4'-(o-tolylmethylene)bis(3-bromo-*N*,*N*-dimethylaniline) (200 mg, 0.4 mmol, 1 eq) was dissolved in anhydrous THF (10 mL) and the reaction temperature was lowered to -78 °C. After stirring at this temperature for 5 min, *sec*-Butyllithium (1.4 M in cyclohexane, 626 µL, 2.2 eq) was added dropwise and the reaction was further stirred for 1h. Silicon tetrachloride (48 µL, 0.42 mmol. 1.05 eq) was then added slowly and the reaction was stirred for 3 h at the same temperature. The temperature was slowly raised to 0 °C by replacing the acetone/dry ice bath with an ice bath and the reaction was left overnight. The next morning, TBAOH (1 M in methanol, 995 µL, 2.5 eq) was added dropwise and the reaction was left for 1 h at room temperature before HCl (2N, 10 mL) was added. The reaction pH was adjusted to between 2 and 3 by saturated sodium bicarbonate solution and DCM was used for extraction. The organic layer was discarded and the aqueous layer pH was further increased to ~7 by adding more sodium bicarbonate solution followed by extraction with DCM. The organic layer was collected, dried over sodium sulfate, and filtered. After removing the solvent, the crude was passed through a short silica column to remove impurities. The resulting beige solid (54 mg) was dissolved in DCM (10 mL) followed by the addition of p-chloranil (164 mg). After 10 min, the reaction temperature was lowered to 0 °C. The solution was filtered, washed with cold DCM, and the solvent was removed. The crude was dissolved in 8 mL HPLC buffer solution (50% acetonitrile / water with 0.1 % trifluoroacetic acid), centrifuged, and purified by HPLC. After lyophilization, 42 mg of a dark blue solid (yield: 20.3 %) was obtained.

Silanediols are known to form disiloxanediols or higher order siloxanes, especially in the absence of bulky neighboring groups.[12] While characterizing **SiOH2R**, we observed the formation of disiloxanediols as well as higher order siloxanes in aprotic solvents such as DCM (see mass spectrometry data immediately below). In protic organic solvents such as ethanol, substitution products containing ethoxy substituents were observed. However, both these processes could be blocked by using water as the solvent. In addition to these observations, previous work has also shown that silanediols can hydrogen bond with anions like acetate.[13] Indeed, NMR titration experiments with increasing amounts of tetrabutylammonium acetate (TBA Ac) in a solution of **SiOH2R** in $CDCl_3$ enabled the resolution of **SiOH2R** proton signals

(see NMR titration data immediately below). Therefore, ^{1}H NMR characterization was performed with the addition of TBA Ac ([**SiOH2R**] = 5 mM, [**SiOH2R**] : [TBA Ac]= 1 : 9.3). Unfortunately, the addition of excess TBA prohibited analysis of **SiOH2R** by ^{13}C NMR.

^{1}H NMR (300 MHz, $CDCl_3$) δ 7.62 (d, *J* = 3.0 Hz, 2H), 7.36 (d, *J* = 7.0 Hz, 1H), 7.30 (s, 1H), 7.25 (s, 1H), 7.03 (d, *J* = 7.4 Hz, 1H), 6.95 (s, 1H), 6.92 (s, 1H), 6.46 (d, *J* = 2.9 Hz, 1H), 6.43 (d, *J* = 3.0 Hz, 1H), 3.28 (s, 12H), 2.01 (s, 3H).

HRMS (EI) m/z calculated for $C_{24}H_{27}N_2O_2Si^+$ $[M]^+$ 403.1836, found 403.1838.

In Water (with 0.5% DMSO)

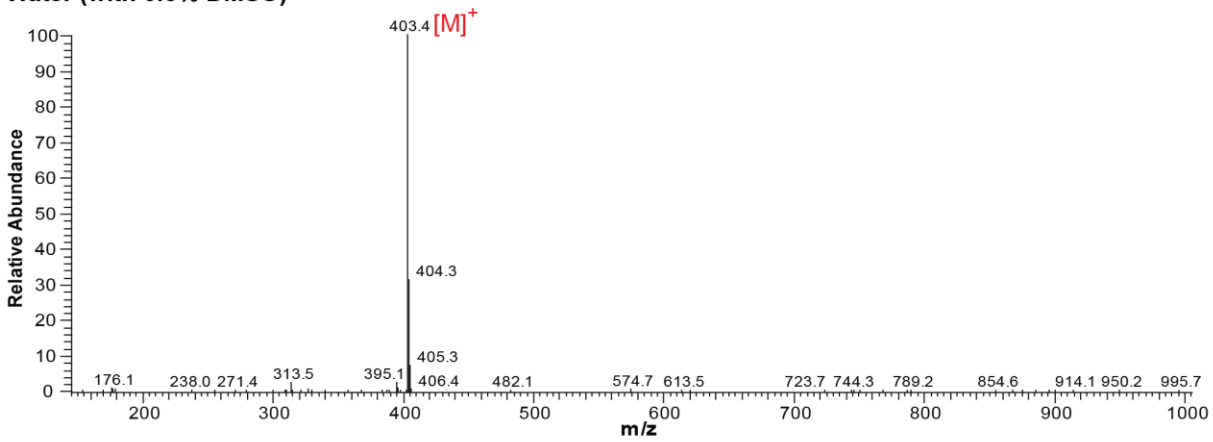

In Ethanol

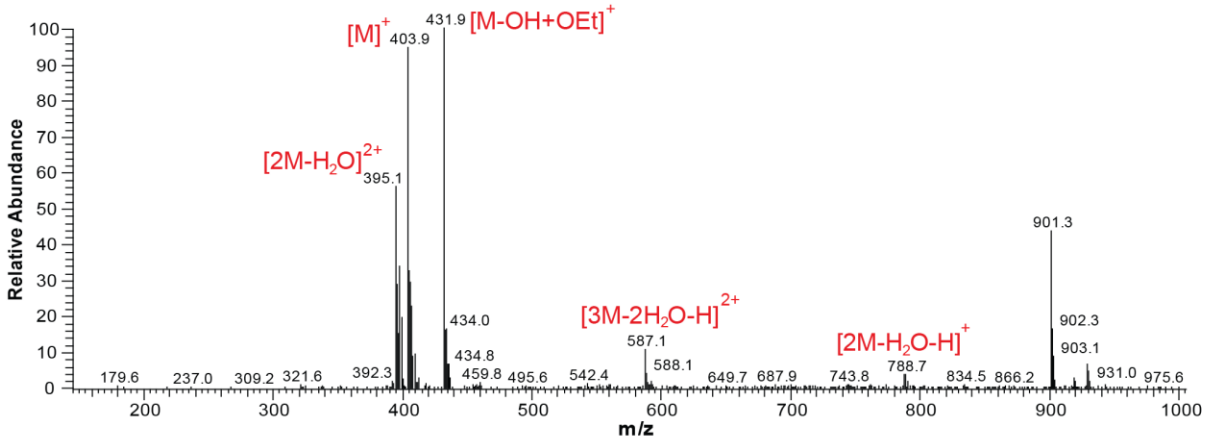

In Dichloromethane

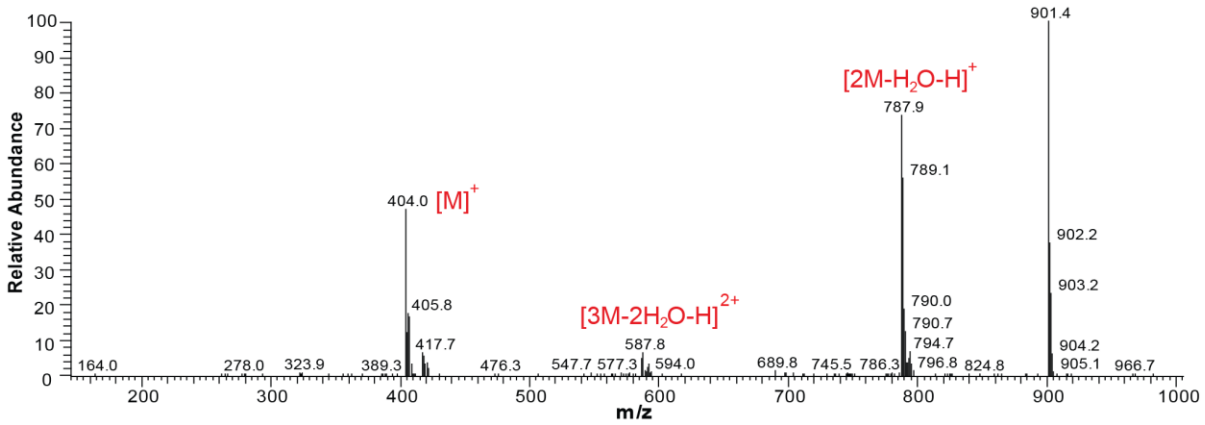

Mass spectrometry data showing **SiOH2R** condensation in different solvents. No evidence of condensation is observed in water.

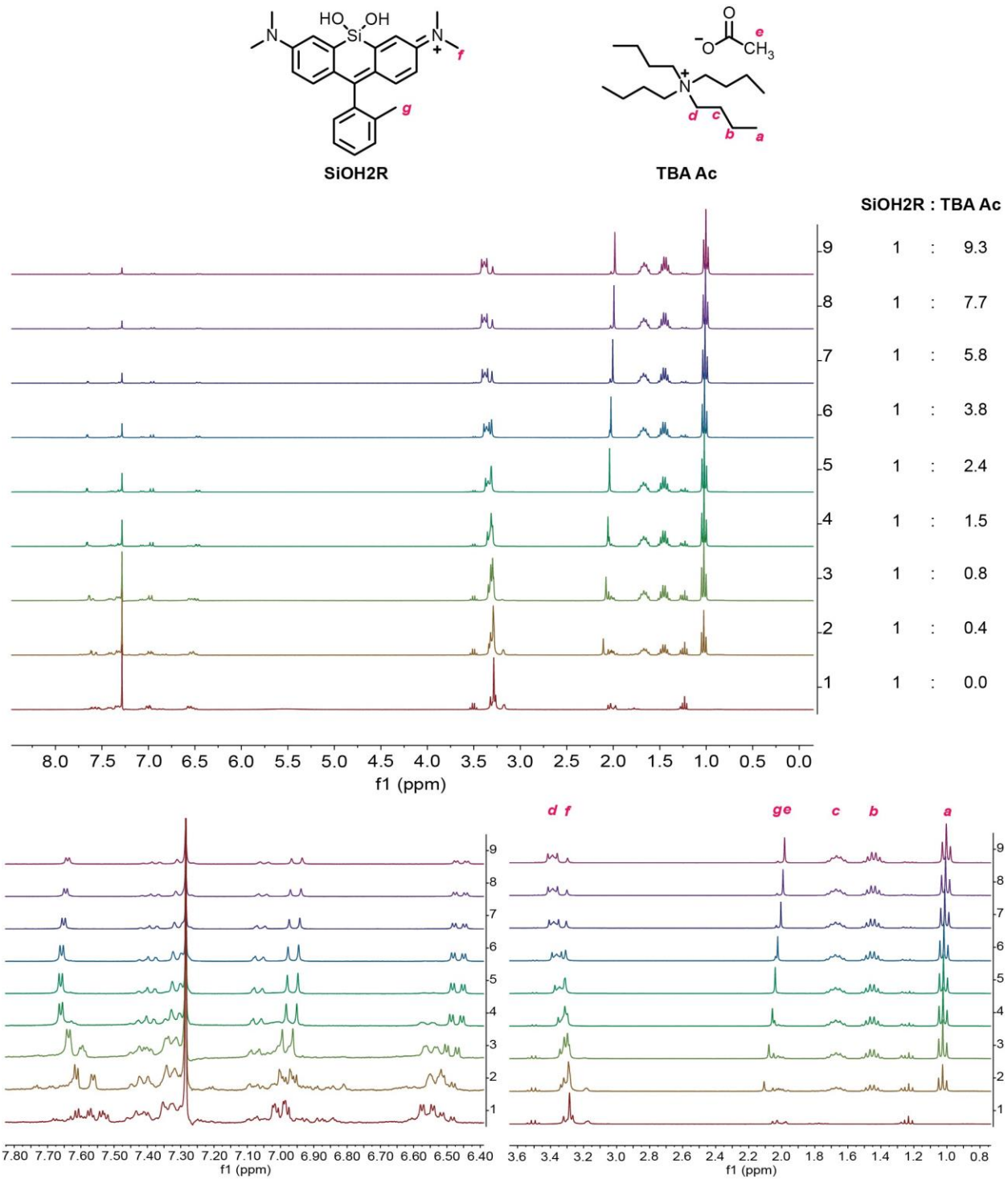

NMR titration indicates silanediol binding with acetate. The ratio between **SiOH2R** and TBA Ac was calculated using peak integration data. TBA Ac allows for the resolution of **SiOH2R** proton signals.

Computational Results

I. **RF_{620} calculation results**

a. The FixSol/TD-B3LYP/6-31++G(d,p) excitation energies for **RF_{620}** at S_0 ground state geometry. There are two transitions, S_0->S_1 at 2.136 eV with an oscillator strength 1.422 and S_0->S_7 at 3.628 eV with an oscillator strength 0.175:

STATE	ENERGY	EXCITATION	TRANSITION DIPOLE, A.U.			OSCILLATOR
0 ->	HARTREE	EV	X	Y	Z	STRENGTH
0 A	-1215.0504956249	0.000				
1 A	-1214.9720064082	2.136	-5.1235	-0.0428	-0.9568	1.4216
2 A	-1214.9515207454	2.693	0.6596	-0.0294	0.0447	0.0289
3 A	-1214.9324574650	3.212	0.2092	-0.4097	0.2402	0.0212
4 A	-1214.9287492870	3.313	0.0773	0.0622	0.0090	0.0008
5 A	-1214.9267934030	3.366	0.1084	0.9945	0.1306	0.0839
6 A	-1214.9194266176	3.567	0.2649	0.3973	0.1528	0.0220
7 A	-1214.9171791894	3.628	0.1535	-1.3843	-0.1836	0.1754
8 A	-1214.9107165549	3.804	-0.0764	-0.3005	0.1560	0.0112
9 A	-1214.8975377204	4.162	-0.0750	-0.7287	-0.2171	0.0595
10 A	-1214.8957361238	4.211	0.9634	-0.0171	0.1466	0.0980

b. The $S_0 \rightarrow S_1$ transition for **RF_{620}** is mainly between MO103 (HOMO) and MO104 (LUMO):

STATE # 1 ENERGY = 2.135800 EV

OSCILLATOR STRENGTH = 1.421556

LAMBDA DIAGNOSTIC = 0.680 (RYDBERG/CHARGE TRANSFER CHARACTER)

SYMMETRY OF STATE = A

		EXCITATION	DE-EXCITATION
OCC	VIR	AMPLITUDE	AMPLITUDE
I	A	X(I->A)	Y(A->I)
---	---	--------	--------
102	104	0.066077	0.000921
103	104	0.996463	-0.078245

c. The FixSol/TD-B3LYP/6-31++G(d,p) fluorescent de-excitation energy (S_1->S_0) for **RF_{620}** at the optimized S_1 state geometry is 2.061 eV with an oscillator strength 1.300:

STATE	ENERGY	EXCITATION	TRANSITION DIPOLE, A.U.	OSCILLATOR

0 ->	HARTREE	EV	X	Y	Z	STRENGTH
0 A	-1215.0488942615	0.000				
1 A	-1214.9731369943	2.061	4.9854	0.0309	0.9391	1.2998

II. **SiOH2R calculation results**

a. The FixSol/TD-B3LYP/6-31++G(d,p) excitation energies for **SiOH2R** at S_0 ground state geometry. There are four transitions, S_0->S_1 at 1.975 eV with an oscillator strength 1.346, S_0->S_4 at 3.251 eV with an oscillator strength 0.228, S_0->S_8 at 3.859 eV with an oscillator strength 0.284 and S_0->S_9 at 4.257 eV with an oscillator strength 0.201:

STATE	ENERGY	EXCITATION	TRANSITION DIPOLE, A.U.			OSCILLATOR
	HARTREE	EV	X	Y	Z	STRENGTH
0 A	-1479.5399157413	0.000				
1 A	-1479.4673396086	1.975	-5.1943	0.0639	-0.9114	1.346
2 A	-1479.4351602108	2.851	-0.0919	0.0645	-0.0135	0.001
3 A	-1479.4270873160	3.070	0.0977	-0.1880	-0.0150	0.003
4 A	-1479.4204379425	3.251	0.0249	-1.6505	-0.3657	0.228
5 A	-1479.4119460853	3.482	-0.8077	0.0481	-0.1395	0.058
6 A	-1479.4055717533	3.656	0.0277	0.3692	-0.0378	0.012
7 A	-1479.3996911537	3.816	-0.4559	0.0316	-0.0464	0.020
8 A	-1479.3980910875	3.859	-1.7022	-0.0143	-0.3221	0.284
9 A	-1479.3834825731	4.257	-0.0401	1.3779	0.1667	0.201
10 A	-1479.3739738310	4.516	0.0452	-0.2618	0.0529	0.008

b. The $S_0 \rightarrow S_1$ transition for **SiOH2R** is mainly between MO107 (HOMO) and MO108 (LUMO):

STATE # 1 ENERGY = 1.974897 EV

OSCILLATOR STRENGTH = 1.345814

LAMBDA DIAGNOSTIC = 0.680 (RYDBERG/CHARGE TRANSFER CHARACTER)

SYMMETRY OF STATE = A

		EXCITATION	DE-EXCITATION
OCC	VIR	AMPLITUDE	AMPLITUDE
I	A	X(I->A)	Y(A->I)
---	---	--------	--------
100	108	-0.040601	0.003328
103	108	-0.031627	-0.003545
107	108	0.999156	-0.088899

c. The FixSol/TD-B3LYP/6-31++G(d,p) fluorescent de-excitation energy (S_1->S_0) for **SiOH2R** at the optimized S_1 state geometry is 1.912 eV with an oscillator strength 1.280:

STATE	ENERGY	EXCITATION	TRANSITION DIPOLE, A.U.			OSCILLATOR
0 ->	HARTREE	EV	X	Y	Z	STRENGTH
0 A	-1479.5387519832	0.000				
1 A	-1479.4684691123	1.912	-5.1474	0.0669	-0.9087	1.2804

III. **SiR calculation results**

a. The FixSol/TD-B3LYP/6-31++G(d,p) excitation energies for **SiR** at S_0 ground state geometry. There are four transitions, S_0->S_1 at 2.054 eV with an oscillator strength 1.428, S_0->S_5 at 3.500 eV with an oscillator strength 0.145, S_0->S_7 at 4.001 eV with an oscillator strength 0.196 and S_0->S_9 at 4.234 eV with an oscillator strength 0.227:

STATE	ENERGY	EXCITATION	TRANSITION DIPOLE, A.U.			OSCILLATOR
	HARTREE	EV	X	Y	Z	STRENGTH
0 A	-1407.6348130267	0.000				
1 A	-1407.5593421841	2.054	5.2301	0.1065	1.0046	1.428
2 A	-1407.5253359904	2.979	-0.0424	-0.0412	-0.0020	0.000
3 A	-1407.5167776701	3.212	-0.2550	0.3516	-0.0087	0.015
4 A	-1407.5144864906	3.274	0.0240	1.0449	0.0973	0.088
5 A	-1407.5061787881	3.500	0.0864	-1.2661	-0.2864	0.145
6 A	-1407.5029592405	3.588	-0.5115	-0.0549	-0.1115	0.024
7 A	-1407.4877744080	4.001	-1.3867	-0.0689	-0.2737	0.196
8 A	-1407.4841714281	4.099	-0.1492	-0.0096	-0.0249	0.002
9 A	-1407.4791983819	4.234	-0.1454	1.4399	0.3113	0.227
10 A	-1407.4771478695	4.290	-0.0733	-0.0517	0.2877	0.010

b. The S_0→S_1 transition for **SiR** is mainly between MO107 (HOMO) and MO108 (LUMO):

STATE # 1 ENERGY = 2.053666 EV

OSCILLATOR STRENGTH = 1.427655

LAMBDA DIAGNOSTIC = 0.679 (RYDBERG/CHARGE TRANSFER CHARACTER)

SYMMETRY OF STATE = A

		EXCITATION	DE-EXCITATION
OCC	VIR	AMPLITUDE	AMPLITUDE
I	A	X(I->A)	Y(A->I)
---	---	---	---
99	108	0.035395	-0.004659

107	108	-0.999197	0.083573

c. The FixSol/TD-B3LYP/6-31++G(d,p) fluorescent de-excitation energy (S_1->S_0) for **SiR** at the optimized S_1 state geometry is 2.000 eV with an oscillator strength 1.378:

STATE	ENERGY	EXCITATION	TRANSITION DIPOLE, A.U.			OSCILLATOR
	HARTREE	EV	X	Y	Z	STRENGTH
0 A	-1407.6338080938	0.000				
1 A	-1407.5603139856	2.000	5.2062	0.0982	1.0009	1.378

IV. **TMR calculation results**

Details concerning these calculations have been previously described.[11]

Figure S1

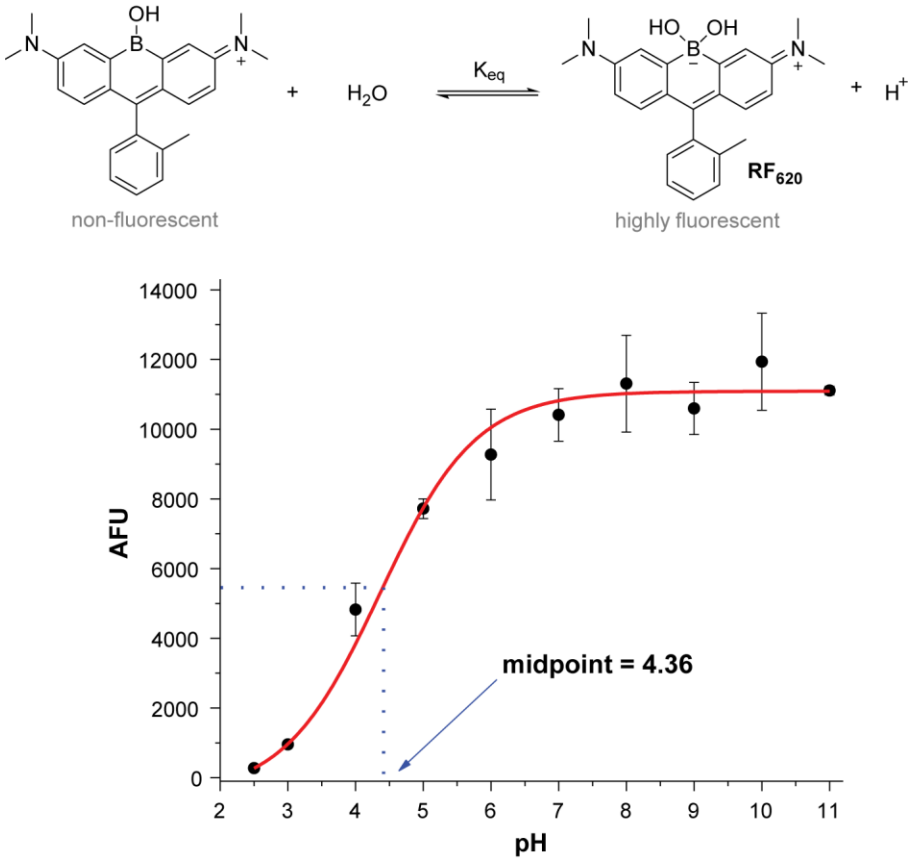

RF_{620} fluorescence emission intensity as a function of different pHs in Britton-Robinson buffer. A midpoint at pH = 4.36 was observed, indicating that **RF_{620}** was present in the fluorescent borinate form under physiological conditions (pH = 7.4).

Figure S2

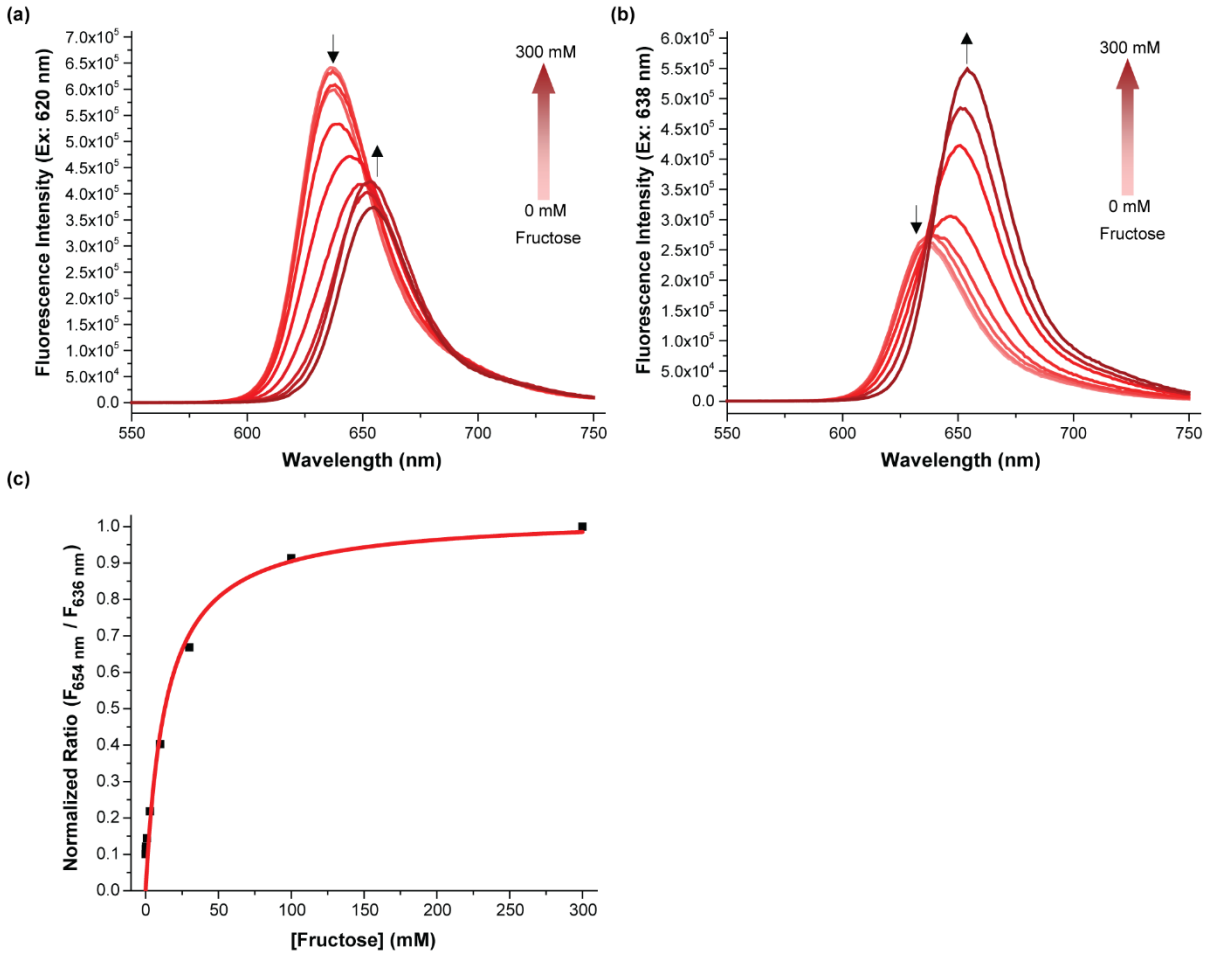

Measurement of the affinity of **RF_{620}** and fructose. (a) Emission spectra upon adding various concentrations of fructose (excitation wavelength: 620 nm). (b) Emission spectra upon adding various concentrations of fructose (excitation wavelength: 638 nm). (c) The dissociation constant was determined by plotting the ratiometric change in fluorescence against the concentration of fructose using: fluorescence ratio = B_{max} * [fructose] / (K_D + [fructose]), where B_{max} = 1.03 ± 0.07 and K_D = 13.95 ± 3.84 mM (R^2 = 1).

Figure S3

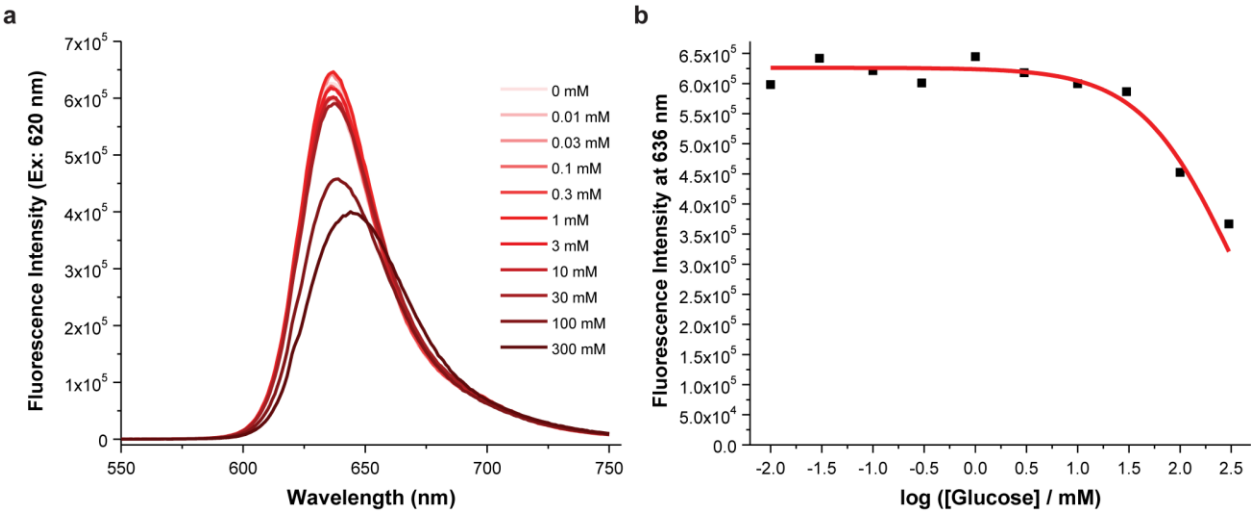

RF_{620} displays relatively weak binding to glucose. (a) Emission spectra upon adding various concentrations of glucose to **RF_{620}** (5 μM, excitation wavelength: 620 nm). (b) By plotting the fluorescence emission at 636 nm against the concentration of glucose, the dissociation constant was estimated to be above 300 mM.

Figure S4

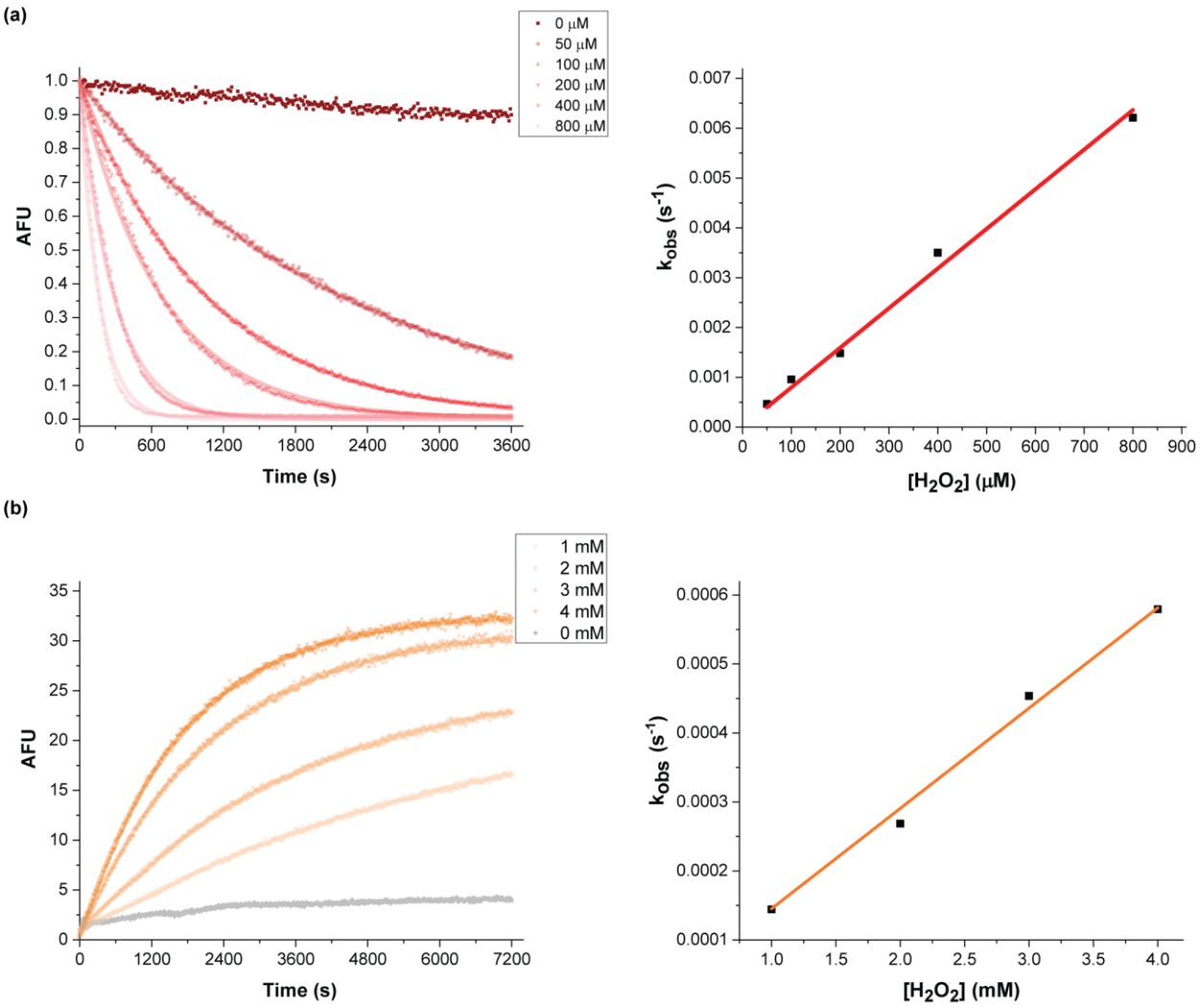

Kinetic measurement of **RF_{620}** reacting with H_2O_2. In order to obtain pseudo first-order kinetics, the concentration of **RF_{620}** was held constant at 5 μM in all experiments; the H_2O_2 concentration was adjusted to be at least 10-fold higher than **RF_{620}**. Data were fit to a first-order equation and the pseudo first-order rate constants were than plotted against concentrations of H_2O_2. The resulting slope of the linear fit yielded the second-order rate constant. (a) **RF_{620}** fluorescence as a function of different concentrations of H_2O_2 (ex: 620 nm, em: 636 nm, left). Linear fit equation: $y = 7.956\times10^{-6} * [H_2O_2]$ ($R^2 = 0.999$, right). (b) TMR formation as function of different concentrations of H_2O_2 (ex: 550 nm, em: 570 nm, left). Linear fit equation: $y = 1.453\times10^{-4} * [H_2O_2]$ ($R^2 = 0.998$, right). Different concentrations of H_2O_2 are used in panels a and b in order to determine rates under experimentally tractable conditions.

Figure S5

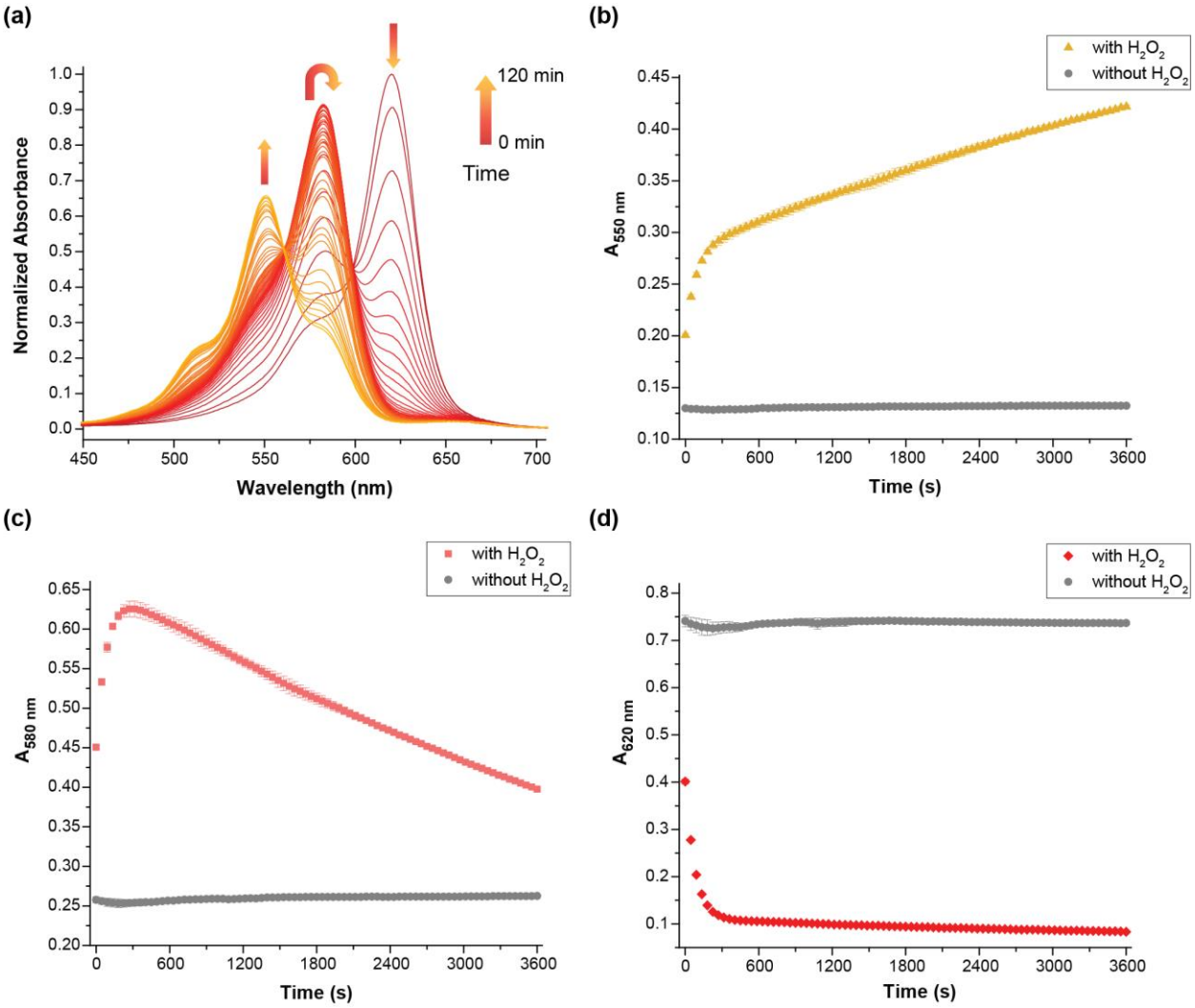

The change in the absorbance spectra of **RF_{620}** (5 μM) reacting with H_2O_2 (2 mM) in PBS (10 mM, pH = 7.4 with 0.5% DMSO) as a function of time. (a) Whole spectra scans show three bands at 550 nm, 580 nm, and 620 nm, which correspond to TMR, an intermediate, and **RF_{620}**. (b) TMR absorbance change at 550 nm over time. (c) Intermediate absorbance change at 580 nm over time. (d) Reactant (**RF_{620}**) absorbance change at 620 nm over time.

Figure S6

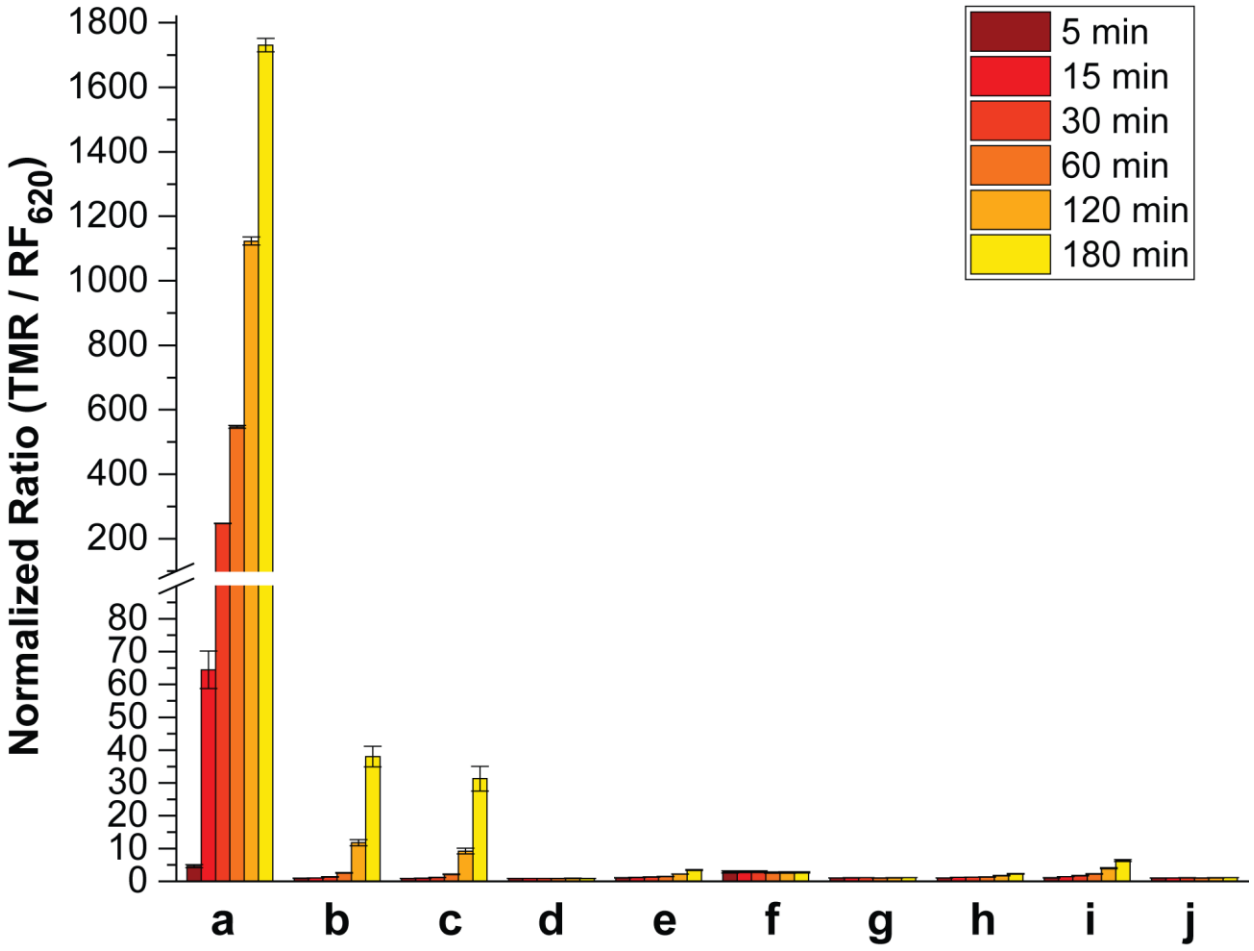

Selectivity of **RF_{620}** (10 μM) against different ROS over time. (a) H_2O_2, (b) superoxide, (c) superoxide with superoxide dismutase (SOD, 15 U/mL), (d) superoxide with catalase (15 U/mL), (e) tert-Butyl hydrogen peroxide (TBHP), (f) HOCl, (g) NO, (h) $\cdot O^tBu$, (i) ·OH, and (j) blank. No formation of TMR is observed in the presence of superoxide and catalase, indicating that superoxide signal is due to decomposition of superoxide to form H_2O_2. The ratio of TMR and **RF_{620}** emission is plotted on the y-axis.

Figure S7

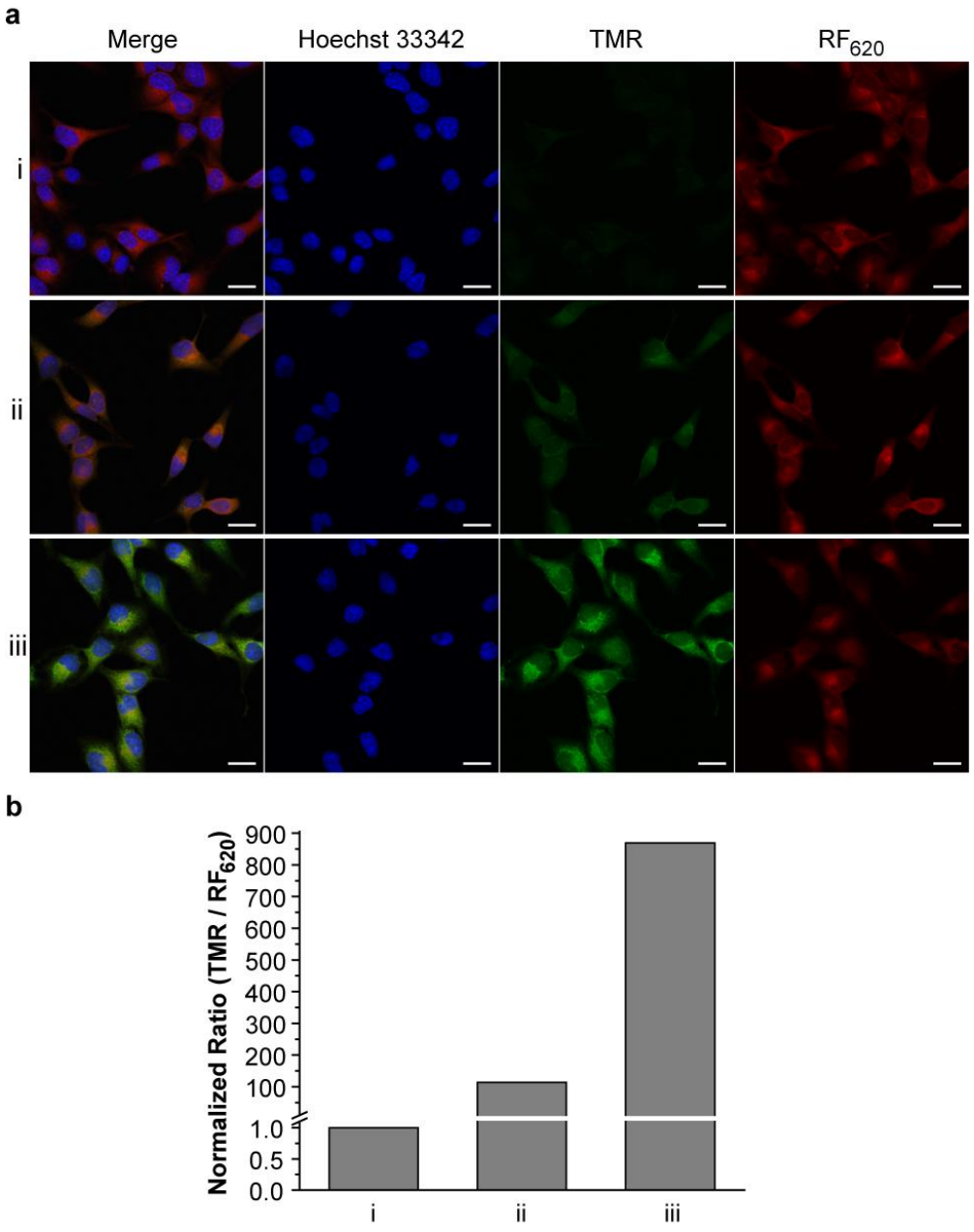

RF_{620} can detect H_2O_2 added exogenously to living cells. (a) Confocal fluorescence microscopy imaging of HeLa cells incubated with i. 0 μM, ii. 40 μM, or iii. 80 μM H_2O_2 for 30 min, washed (3x) and incubated with 10 μM **RF_{620}** for 1 h. (b) Comparison of the ratio between TMR and **RF_{620}** emission. Scale bar: 25 μm.

Figure S8

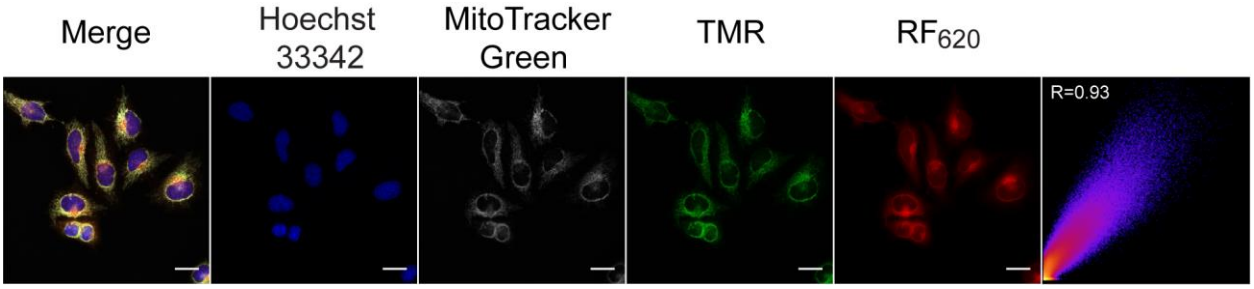

HeLa cells were incubated with **RF_{620}** (10 μM) and stimulated with PMA (1 μg/mL). MitoTracker Green (MTG, 100 nM) colocalized with TMR formation. A 2D colocalization scatter plot of MTG and TMR fluorescence, with the calculated Pearson's colocalization coefficient, are shown on the right. Scale bar: 25 μm.

Figure S9

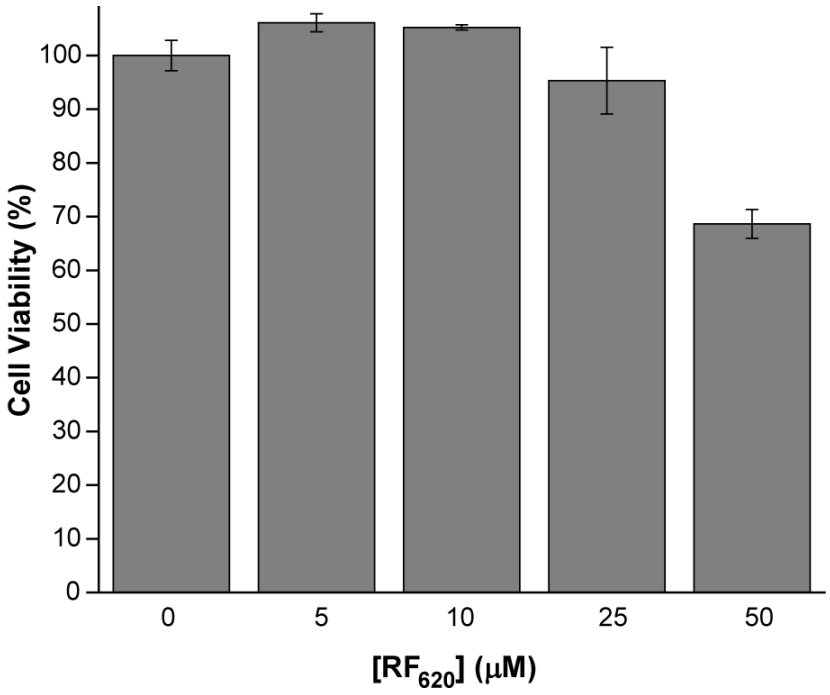

The toxicity of **RF_{620}** was assessed by incubating HeLa cells for 6 h with the dye and measuring viability using the CellTiter-Glo 2.0 Assay (Promega).

Figure S10

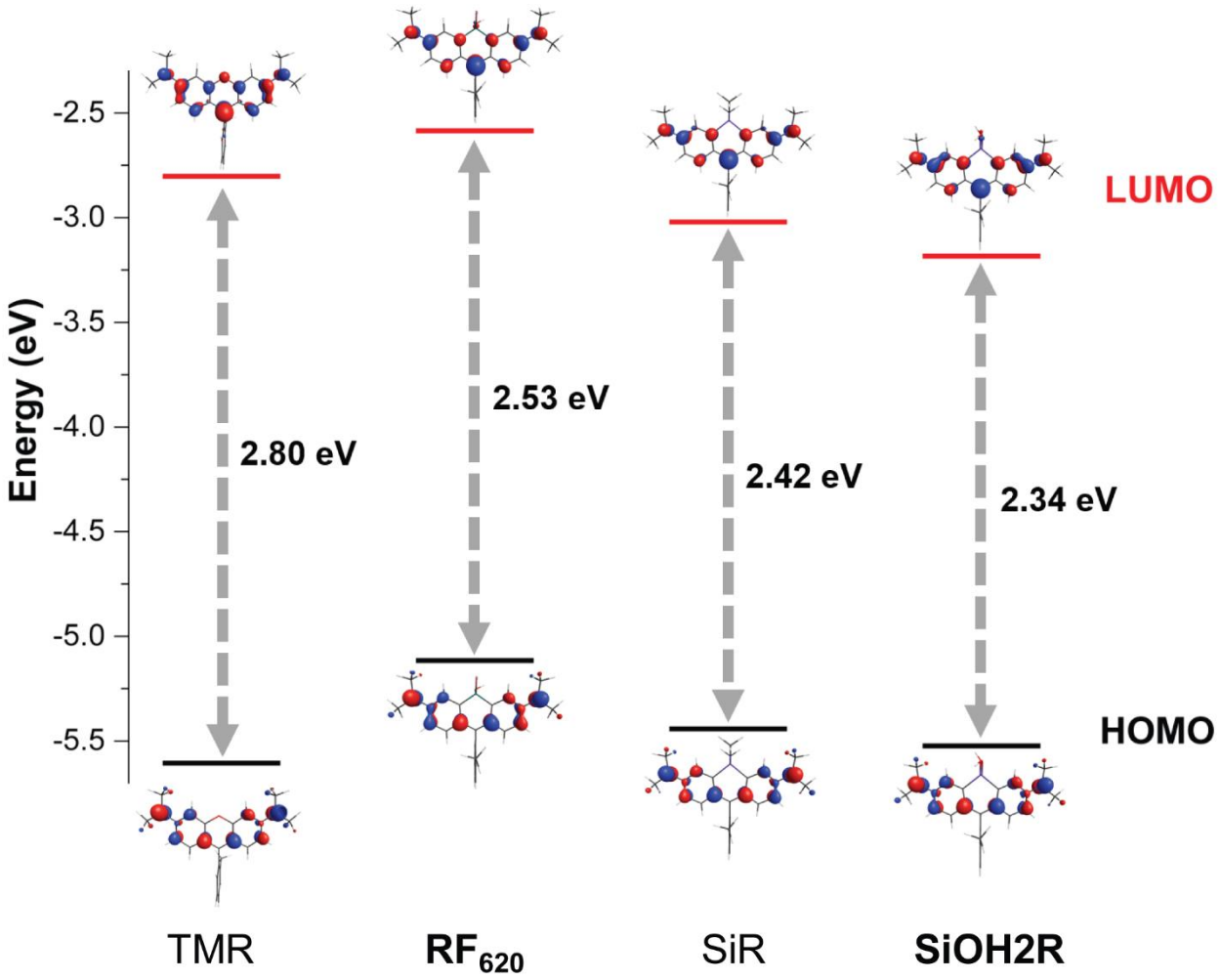

A comparison of computationally calculated molecular orbitals as well as HOMO and LUMO energies of TMR, **RF_{620}**, SiR, and **SiOH2R**.

Figure S11

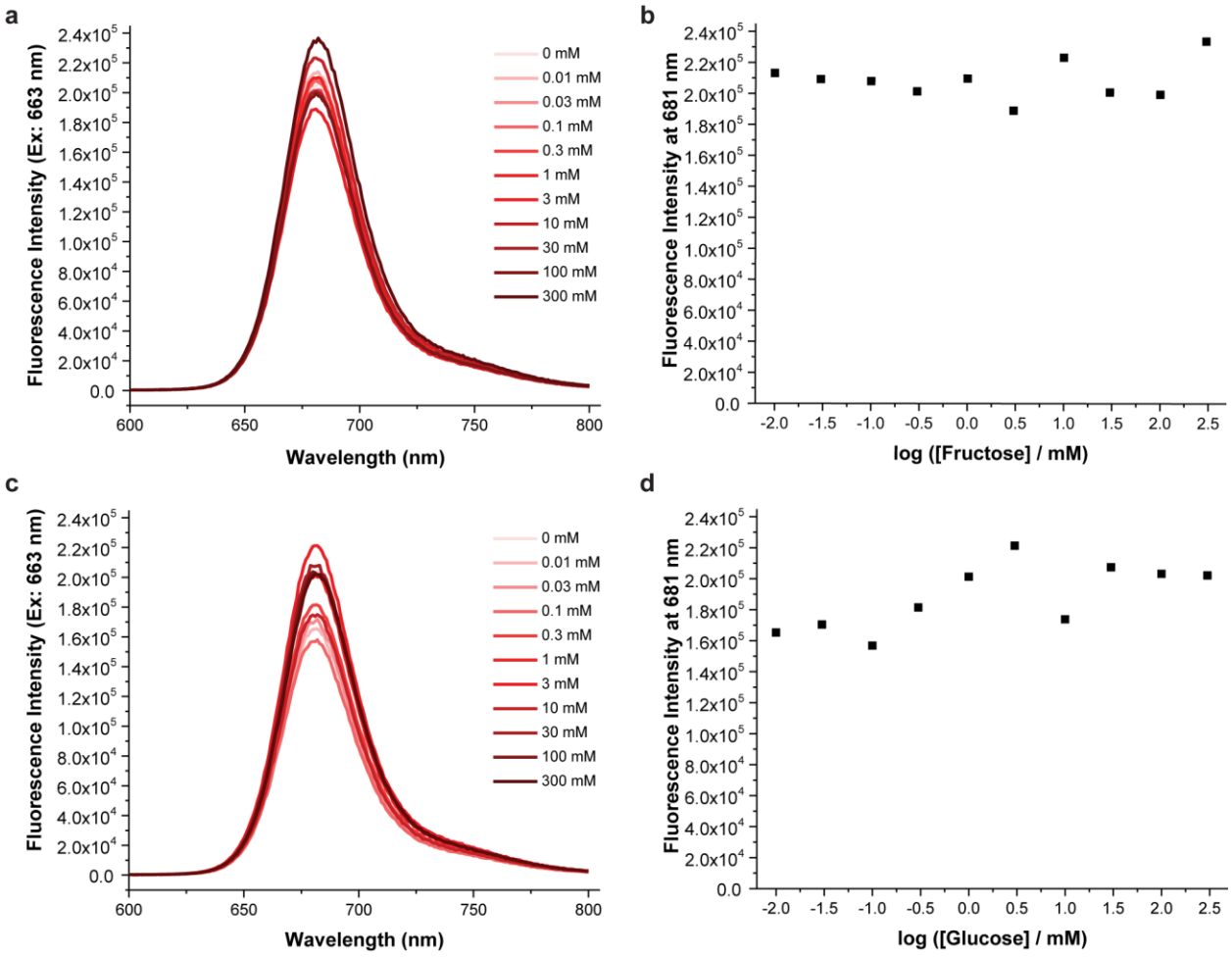

Fructose and glucose do not influence the fluorescence of **SiOH2R**. (a) Emission spectra upon adding various concentrations of fructose to **SiOH2R** (5 μM, excitation wavelength: 663 nm). (b) The fluorescence emission signal at 681 nm plotted against the concentration of fructose. (c) Emission spectra upon adding various concentrations of glucose to **SiOH2R** (5 μM, excitation wavelength: 663 nm). (d) The fluorescence emission signal at 681 nm plotted against the concentration of glucose.

Figure S12

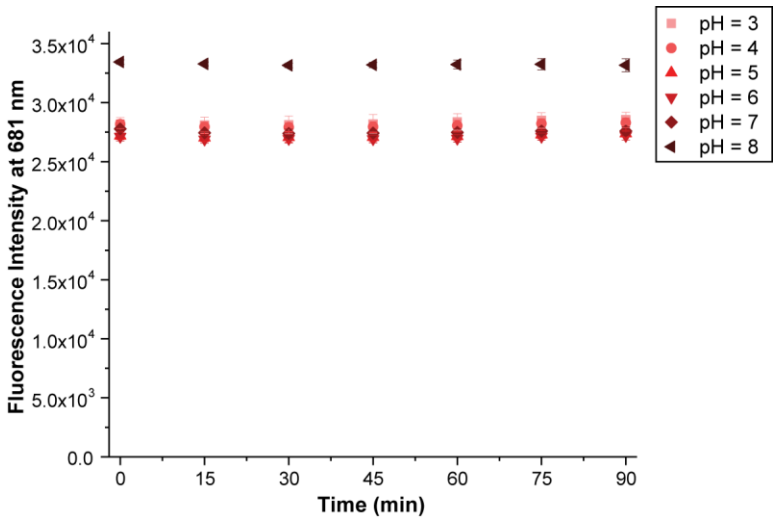

No appreciable change in **SiOH2R** fluorescence is observed at varying pHs. The fluorescence intensity at 681 nm (ex: 663 nm) of **SiOH2R** (10 μM) in solutions of varying pH (Britton-Robinson buffer) were monitored over 90 min in triplicate.

Figure S13

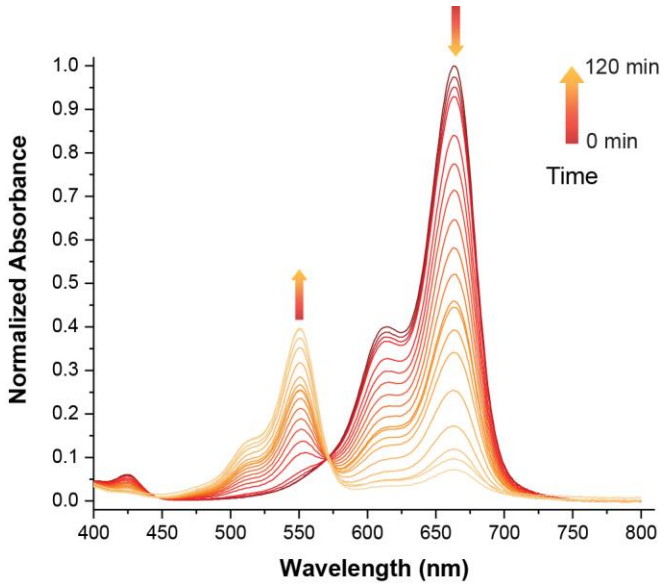

Absorbance spectra of **SiOH2R** (5 μM) reacting with H_2O_2 (2 mM) as a function of time in PBS (10 mM, pH = 8.0, with 0.5% DMSO).

Figure S14

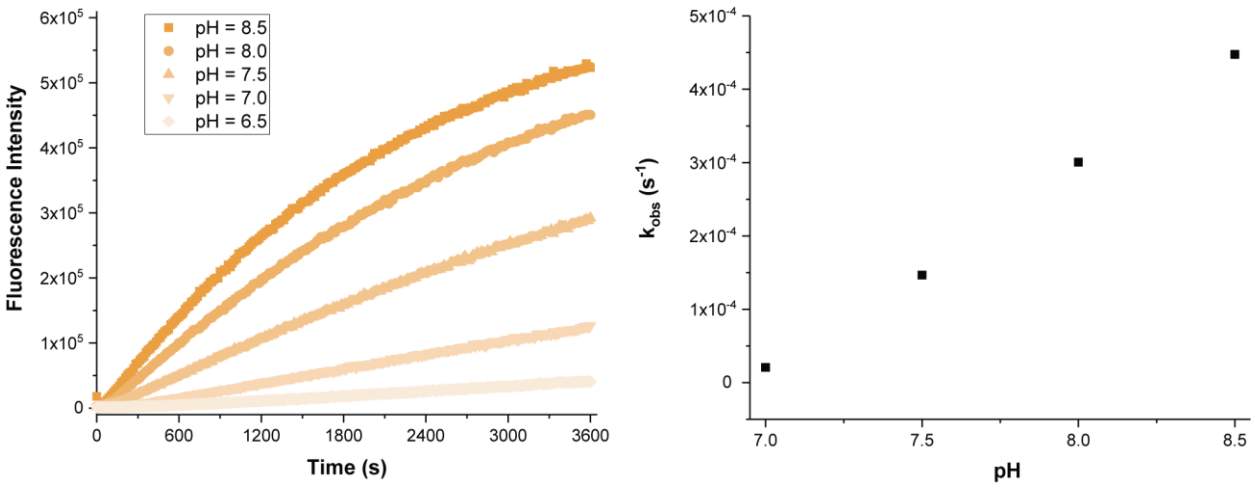

Kinetics of **SiOH2R** (5 µM) reacting with H_2O_2 (2 mM) at different pH (left) and the pseudo first-order rate constants plotted against pH (right).

Figure S15

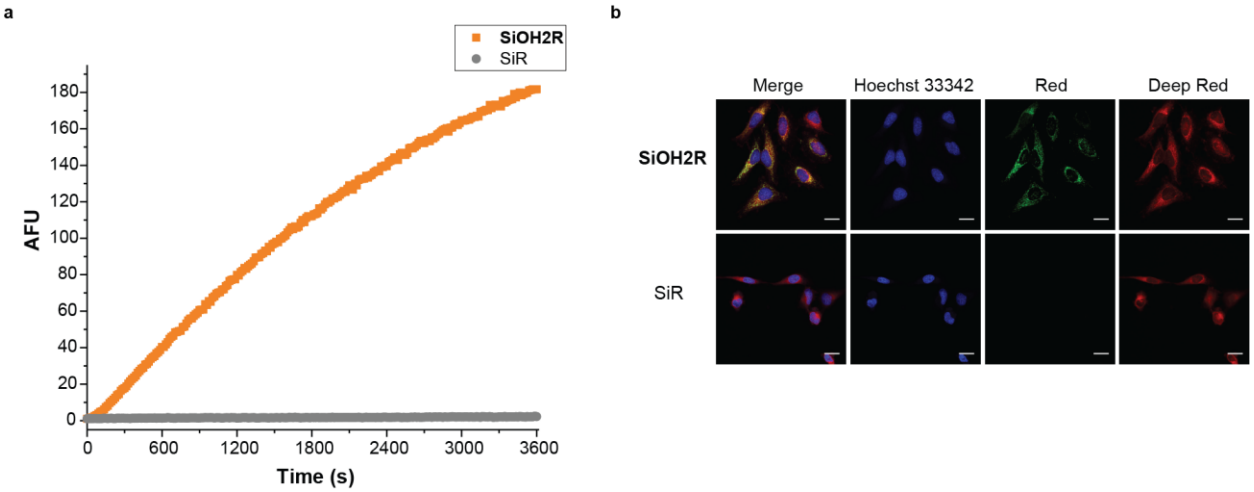

Reactivity comparison of SiR and **SiOH2R** towards H_2O_2. (a) *In vitro* comparison of TMR formation by SiR and **SiOH2R** (5 µM each) in the presence of H_2O_2 (2 mM) in PBS (10 mM, pH = 8.0, with 0.5% DMSO). TMR signal (ex: 550 nm, em: 570 nm) was monitored over time. (b) HeLa cells were incubated with 10 µM of each dye for 30 min, washed (3x), and incubated with H_2O_2 (50 µM) for 1 h and imaged. Scale bar: 25 µm.

Figure S16

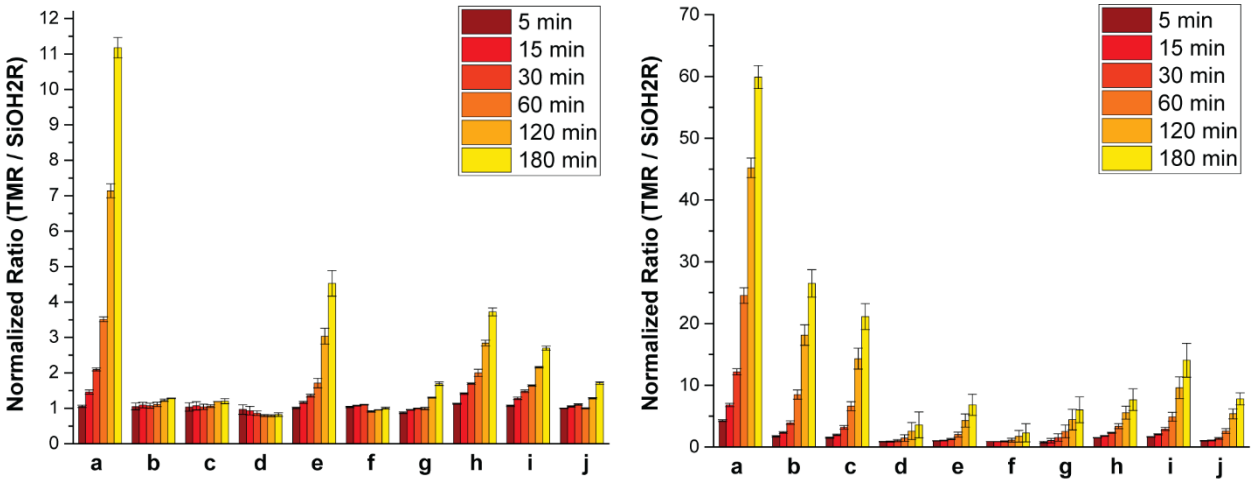

Selectivity of **SiOH2R** (10 μM) against different ROS as a function of time in pH = 7.4 (left) and pH = 8.5 (right). (a) H_2O_2, (b) superoxide, (c) superoxide with superoxide dismutase (SOD, 15 U/mL), (d) superoxide with catalase (15 U/mL), (e) tert-butyl hydrogen peroxide (TBHP), (f) HOCl, (g) NO, (h) $\cdot O^tBu$, (i) $\cdot OH$, and (j) blank. At pH = 8.5, the addition of catalase abolishes the formation of TMR in the presence of superoxide, indicating that superoxide signal is due to decomposition of superoxide to form H_2O_2.

Figure S17

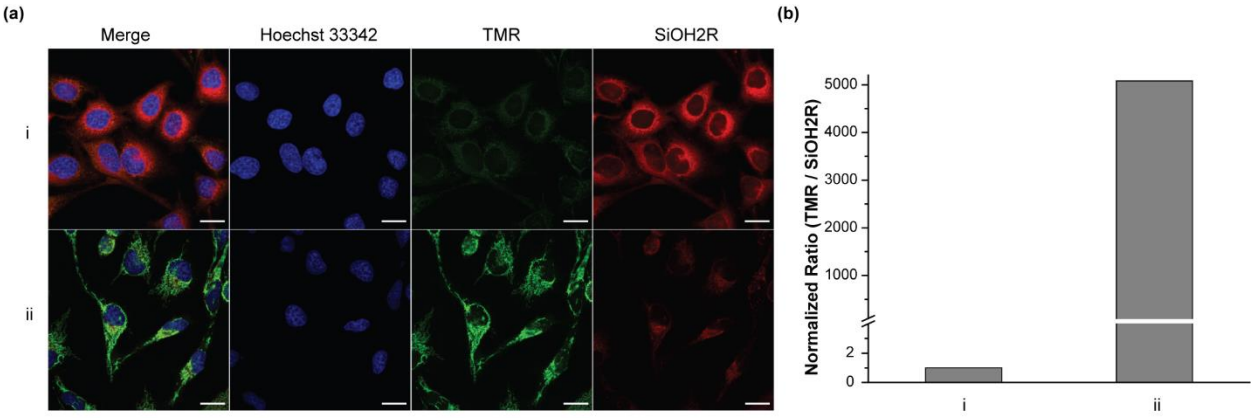

Live cell imaging of serum starved HeLa cells with **SiOH2R** (10 μM) after the addition of exogenous H_2O_2 (80 μM). (a) Images of the TMR (green) and **SiOH2R** (red) channels. i. without H_2O_2 and ii with H_2O_2 (80 μM) incubation for 90 min. Scale bar: 10 μm. (b) The ratio of TMR and **SiOH2R** emission is shown.

Figure S18

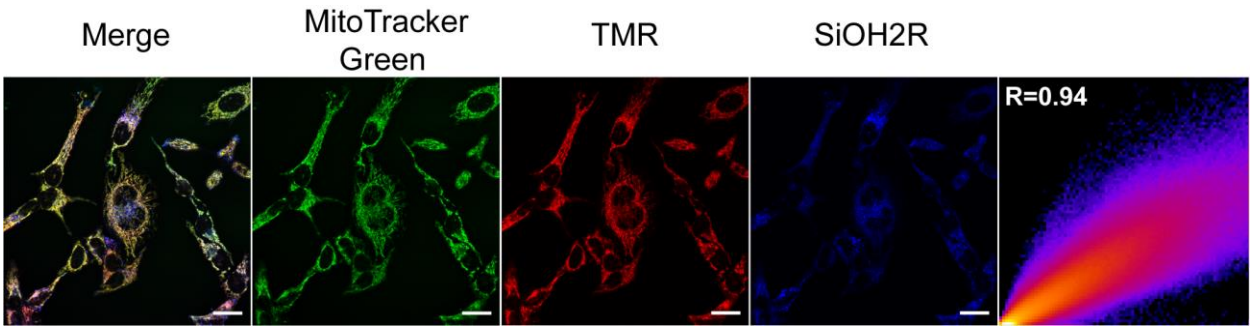

HeLa cells were incubated with **SiOH2R** (10 μM) and stimulated with PMA (1 μg/mL). MitoTracker Green (MTG, 100 nM) colocalized with TMR formation. A 2D colocalization scatter plot of MTG and TMR fluorescence, with the calculated Pearson's colocalization coefficient, are shown on the right. Scale bar: 25 μm.

Figure S19

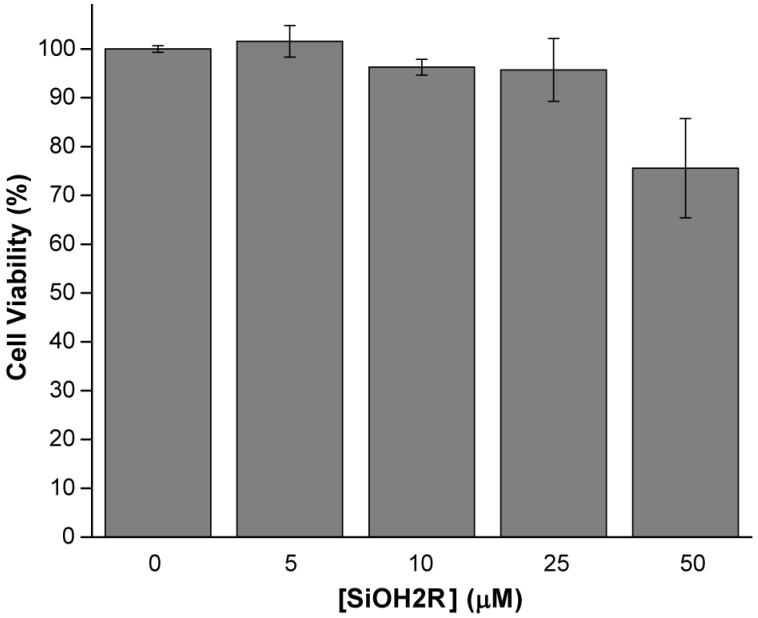

The toxicity of **SiOH2R** was assessed by incubating HeLa cells for 6 h with the dye and measuring viability with the CellTiter-Glo 2.0 Assay (Promega).

Copies of ^{1}H, ^{13}C and ^{11}B NMR Spectra

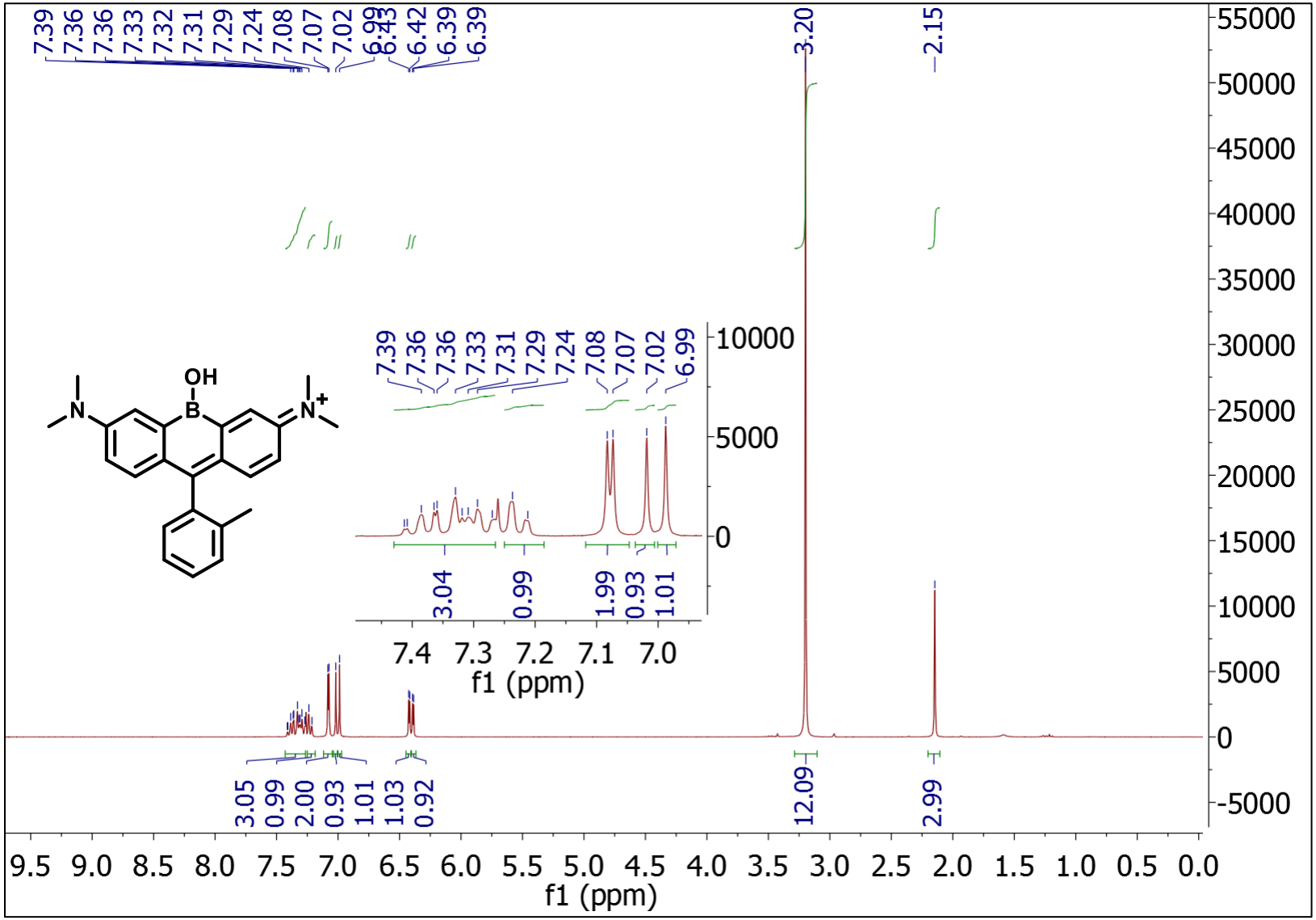

^{1}H NMR chart of **RF_{620}** (borinic acid form) in $CDCl_3$ (300 MHz).

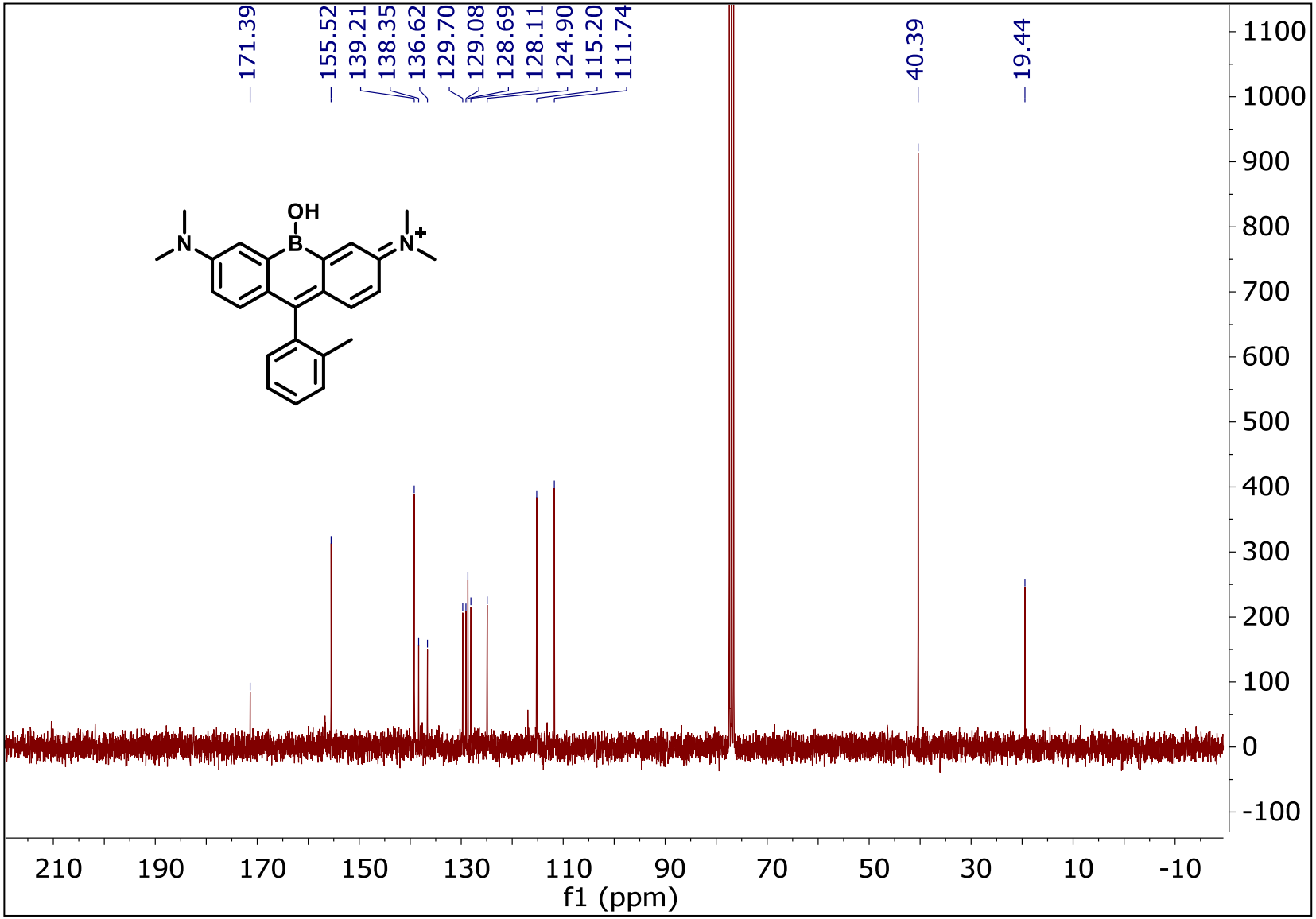

^{13}C NMR chart of **RF$_{620}$** (borinic acid form) in $CDCl_3$ (75 MHz).

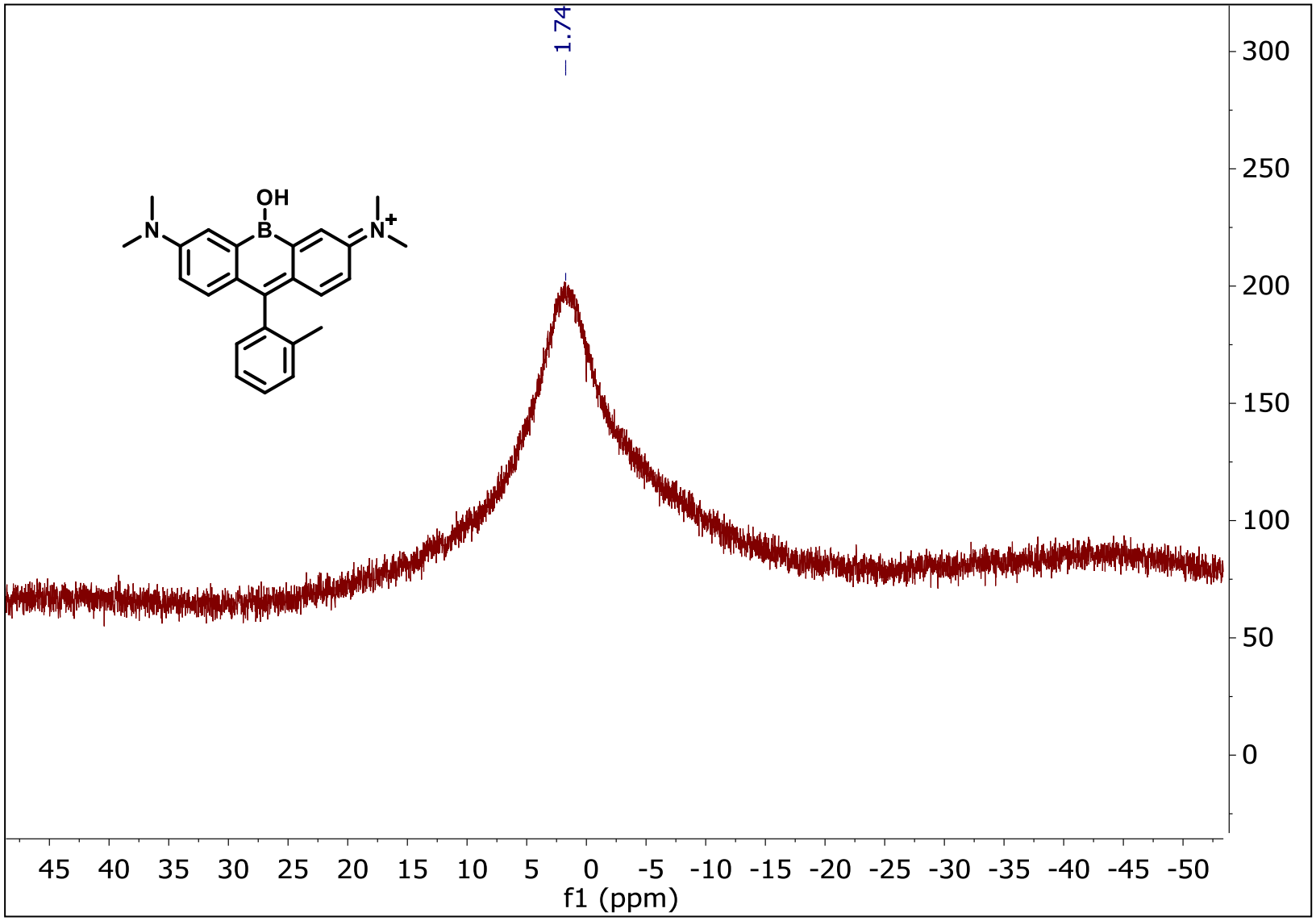

^{11}B NMR chart of **RF$_{620}$** (borinic acid form) in $CDCl_3$ (96 MHz).

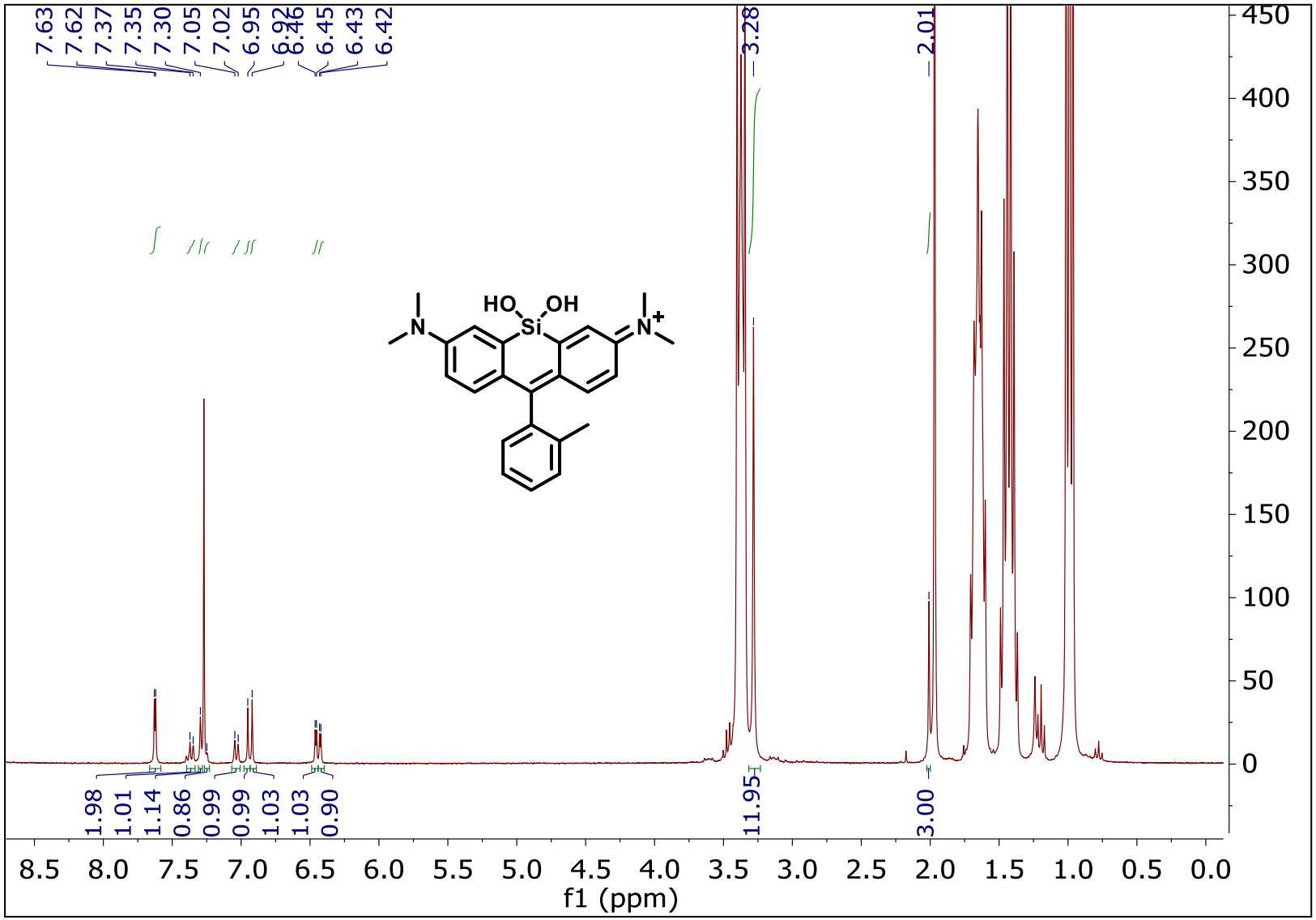

^{1}H NMR chart of **SiOH2R** (with TBA Ac) in $CDCl_3$ (300 MHz).

References

[1] D. Bradley, G. Williams, M. Lawton, *J. Org. Chem.* **2010**, *75*, 8351-8354.

[2] a) M. E. Casida, in *Recent Advances in Density Functional Methods* (Ed.: D. P. Chong), World Scientific, Singapore, **1995**, p. 155; b) M. E. Casida, C. Jamorski, K. C. Casida, D. R. Salahub, *J. Chem. Phys.* **1998**, *108*, 4439-4449.

[3] N. M. Thellamurege, D. Si, F. Cui, H. Zhu, R. Lai, H. Li, *J. Comput. Chem.* **2013**, *34*, 2816-2833.

[4] a) M. S. Gordon, M. W. Schmidt, *Theory and Applications of Computational Chemistry: the first forty years* **2005**, 1167-1189; b) M. W. Schmidt, K. K. Baldridge, J. A. Boatz, S. T. Elbert, M. S. Gordon, J. H. Jensen, S. Koseki, N. Matsunaga, K. A. Nguyen, S. Su, *J. Comput. Chem.* **1993**, *14*, 1347-1363.

[5] A. D. Becke, *J. Chem. Phys.* **1993**, *98*, 5648-5652.

[6] M. M. Francl, W. J. Pietro, W. J. Hehre, J. S. Binkley, M. S. Gordon, D. J. DeFrees, J. A. Pople, *J. Chem. Phys.* **1982**, *77*, 3654-3665.

[7] N. M. Thellamurege, H. Li, *J. Chem. Phys.* **2012**, *137*, 246101.

[8] A. M. Brouwer, *Pure Appl. Chem.* **2011**, *83*, 2213-2228.

[9] K. Rurack, M. Spieles, *Anal. Chem.* **2011**, *83*, 1232-1242.

[10] a) D. Srikun, E. W. Miller, D. W. Dornaille, C. J. Chang, *J. Am. Chem. Soc.* **2008**, *130*, 4596-4597; b) X. Sun, Q. Xu, G. Kim, S. E. Flower, J. P. Lowe, J. Yoon, J. S. Fossey, X. Qian, S. D. Bull, T. D. James, *Chem. Sci.* **2014**, *5*, 3368-3373.

[11] X. Zhou, R. Lai, J. R. Beck, H. Li, C. I. Stains, *Chem. Commun.* **2016**, *52*, 12290-12293.

[12] a) N. T. Tran, T. Min, A. K. Franz, *Chem. Eur. J.* **2011**, *17*, 9897-9900; b) A. G. Schafer, J. M. Wieting, A. E. Mattson, *Org. Lett.* **2011**, *13*, 5228-5231.

[13] S. Kondo, T. Harada, R. Tanaka, M. Unno, *Org. Lett.* **2006**, *8*, 4621-4624.